4-19-2006

Morphology and Properties of Soy Protein and Polylactide Blends

Jinwen Zhang
Washington State University

Long Jiang
Washington State University

Linyoung Zhu
Washington State University

Jay-Lin Jane
Iowa State University, jjane@iastate.edu

Perminus Mungara
Iowa State University

Morphology and Properties of Soy Protein and Polylactide Blends

Abstract
Blends of soy protein (SP) and a semicrystalline polylactide (PLA) were prepared using a twin-screw extruder. The melt rheology, phase morphology, mechanical properties, water resistance, and thermal and dynamic mechanical properties were investigated on specimens prepared by injection molding of these blends. The melt flowability of soy-based plastics was improved through blending with PLA. Scanning electron microscopy revealed that a cocontinuous phase structure existed in the blends with soy protein concentrate (SPC) to PLA ratios ranging from 30:70 to 70:30. SPC/PLA blends showed fine co-continuous phase structures, while soy protein isolate (SPI)/ PLA blends presented severe phase coarsening. At the same SP to PLA ratios, SPC/PLA blends demonstrated a higher tensile strength than SPI/PLA blends. The water absorption of soy plastics was greatly reduced by blending with PLA. The compatibility was improved by adding 1-5 phr poly(2-ethyl-2-oxazoline) (PEOX) in the blends, and the resulting blends showed an obvious increase in tensile strength and a reduction in water absorption for SPI/PLA blends. The compatibility between SP and PLA was evaluated by mechanical testing, dynamic mechanical analysis (DMA), water absorption, and scanning electron microscopy (SEM) experiments. Differential scanning calorimetry (DSC) revealed that PLA in the blends was mostly amorphous in the injection molded articles, and SP accelerated the cold crystallization and could increase the final crystallinity of PLA in the blends.

Keywords
Center for Crop Utilization Research

Comments
Reprinted with permission from *Biomacromolecules* 7(5): 1551-1561. doi: 10.1021/bm050888p. Copyright 2006 American Chemical Society.

Morphology and Properties of Soy Protein and Polylactide Blends

Jinwen Zhang,*,† Long Jiang,† and Linyong Zhu‡

Wood Materials and Engineering Laboratory and Department of Chemistry, Washington State University, Pullman, Washington 99164

Jay-lin Jane and Perminus Mungara

Department of Food Science and Human Nutrition and Center for Crop Utilization Research, Iowa State University, Ames, Iowa 50011

Received November 21, 2005; Revised Manuscript Received March 8, 2006

Blends of soy protein (SP) and a semicrystalline polylactide (PLA) were prepared using a twin-screw extruder. The melt rheology, phase morphology, mechanical properties, water resistance, and thermal and dynamic mechanical properties were investigated on specimens prepared by injection molding of these blends. The melt flowability of soy-based plastics was improved through blending with PLA. Scanning electron microscopy revealed that a co-continuous phase structure existed in the blends with soy protein concentrate (SPC) to PLA ratios ranging from 30:70 to 70:30. SPC/PLA blends showed fine co-continuous phase structures, while soy protein isolate (SPI)/PLA blends presented severe phase coarsening. At the same SP to PLA ratios, SPC/PLA blends demonstrated a higher tensile strength than SPI/PLA blends. The water absorption of soy plastics was greatly reduced by blending with PLA. The compatibility was improved by adding 1−5 phr poly(2-ethyl-2-oxazoline) (PEOX) in the blends, and the resulting blends showed an obvious increase in tensile strength and a reduction in water absorption for SPI/PLA blends. The compatibility between SP and PLA was evaluated by mechanical testing, dynamic mechanical analysis (DMA), water absorption, and scanning electron microscopy (SEM) experiments. Differential scanning calorimetry (DSC) revealed that PLA in the blends was mostly amorphous in the injection molded articles, and SP accelerated the cold crystallization and could increase the final crystallinity of PLA in the blends.

Introduction

As a renewable plant-based polymer, soy protein (SP) has attracted intensive research interests in nonfood industrial applications.[1−5] When adequate water and heat are present, SP can gelate and undergo conventional melt processing like a thermoplastic. However, strong intra- and intermolecular interactions of SP result in high melt viscosity that makes the melt processing, such as extrusion and injection molding, very difficult unless a sufficient amount of plasticizers and processing aids are added.[2−4] Although water serves as an efficient plasticizer during the melt processing of SP, it evaporates during processing and storage. The properties of the resulting products change with the humidity of the environment. Low molecular weight polyols such as glycerol, ethylene glycol, propylene glycol, saccharides, and their derivatives can be used as plasticizers for SP,[2,3,6] but the resulting materials show low mechanical properties due to a significant amount of plasticizers. Other processing aids, such as sodium tripolyphosphate for interrupting soy protein ionic interactions[3,7] or sodium sulfite as a reducing agent to break the disulfide bonds,[8] were also employed. These processing aids do improve the moisture resistance of SP-based plastics. Nevertheless, they have a very limited effect on flowability improvement. Blending SP with other hydrophobic thermoplastics is an alternative to increase the processability and moisture resistance of the SP products. Using a small amount of maleic anhydride (MA) grafted polyesters, the compatibility between SP and several biodegradable polyesters was greatly increased.[9] Methylene diphenyl diisocyanate (MDI) was found to increase the tensile strength of the SP/PCL blends.[10] On the other hand, blends of SP and poly(hydroxyl ester ether) exhibited acceptable mechanical properties without using a compatibilizer, due to strong hydrogen bonding between the two components.[4] SP plasticizing conditions also showed a significant influence on the compatibility between SP and polyester.[11] Other SP plastics, such as SP/PU,[12,13] SP/lignin,[14] and SP/chitin,[15,16] have also been studied.

PLA is a corn starch-based thermoplastic polyester that has attracted extensive studies for biomedical devices and biodegradable plastics. Depending on the L(+)- and D(−)-lactic acid monomer ratio as well as the molecular weight, PLA can be totally amporphous or up to 80% crystalline, showing comparable mechanical strengths to many synthetic polymers. However, its relatively high price, low heat distortion temperature, and postprocess embrittlement remain as major obstacles for broader applications. Therefore, PLA has often been blended with other polymers or mixed with fillers for cost reduction and/or performance improvement (e.g., with starch,[17,18] inorganic fillers,[19] and natural fiber flax[20]).

In this study, blends of SP and PLA were investigated. The main objective of this study was to improve the processibility and water resistance of SP-based plastics through blending with PLA. It was also an attempt of this study to demonstrate that soy protein, the abundant residual from soybean oil crushing, can also be used for PLA blends, as starch has already been used for PLA blends. In this study, morphology, mechanical and thermal properties, and water absorption of the SP/PLA

* Corresponding author. Tel.: (509) 335-8723; e-mail: jwzhang@wsu.edu.
† Wood Materials and Engineering Laboratory.
‡ Department of Chemistry.

10.1021/bm050888p CCC: $33.50
Published on Web 04/19/2006

blends were investigated. Effects of poly(2-ethyl-2-oxazoline) (PEOX) as a compatibilizer for the SP/PLA blends were evaluated. PEOX is regarded as a derivative polymeric homologue of the aprotic polar solvent, *N*,*N*-dimethylacetamide (DMAc), which is considered as a broadly compatible polymeric solvent or compatibilizing agent for many polymers.[21] It shows high miscibility with many synthetic polymers including poly(vinyl chloride), polystyrene, polypropylene,[22] poly(vinyl alcohol),[23] poly(hydroxyl ether of bisphenol A),[24] chitosan,[25] poly(ethylene-*co*-methacrylic acid),[26] etc. PEOX is an amorphous polymer and slightly basic due to its tertiary amide structure.[22] SPI and SPC are usually prepared by precipitation at its isoelectric point (ca. pH 4.5),[1] which makes them slightly acidic. Therefore, the acid−base interaction could contribute to the compatibilization. Other polymer−polymer interactions, such as hydrogen bonding and ion−dipole and dipole−dipole interactions, might also contribute to the reduction of the interfacial tension and the improvement of compatibility.[25−28]

Experimental Procedures

Materials. Two commercial grades of SP, soy protein isolate (SPI) and concentrate (SPC), were used in this study. SPI (Supro 760) was obtained from Protein Technologies International (St. Louis, MO). It contained ca. 92% protein (dry basis), less than 1% carbohydrate, 4.7% moisture, and 4% ash. SPC (Arcon F) was from Archer Daniels Midland Company (Decatur, IL) with a formulation of ca. 69% protein (dry basis), 20% carbohydrate, 3% fat, and 9% moisture. Semicrystalline PLA was a commercial product (Natureworks PLA 4032D, Natureworks) with a weight-average molecular weight of 207 kDa and polydispersity of 1.74. PEOX ($M_w \sim 500\,000$ Da) was obtained from Aldrich. All other chemicals used in this study were of reagent grade. All polymer materials and chemicals were used as received.

Preparation of Blends. SPI or SPC was formulated prior to mixing with PLA and the compatibilizer. The formulated SP contained SPI or SPC (100 parts, dry weight), sodium sulfite (0.5 parts), sodium tripolyphosphate (1 part), lubricant (0.8 parts), glycerol (2 parts), and water (10 parts). The ingredients were mixed in a high speed mixer (Henschel Mixers American, Inc., Houston, TX), stored in sealed plastic bags, and left overnight at room temperature to equilibrate. This preformulated SP, PLA, and PEOX was then compounded using a corotating twin-screw extruder (Leistritz ZSE-18HP) equipped with a volumetric feeder. The diameter of the screw was 17.8 mm with a length-to-diameter ratio (L/D) of 40. Since the preformulated SP contained 10 parts of water, the compounding extrusion temperature was set as low as possible to reduce the degree of PLA hydrolysis. The barrel of the extruder had seven heating zones. From the feeder to the die, the temperatures were set at 90, 100, 125, 145, 160, 160, and 155 °C, respectively. The die temperature was 155 °C, and the screw speed of 60 rpm was employed for all compounding. There is an atmosphere venting port in the third heating zone and a vacuum venting port in the last heating zone. Since the extrudate was fragile, it was discharged to open air and granulated using a granulator afterward. The compounds were then dried at 90 °C for 8 h before injection molding. The blends containing 30:70, 50:50, and 70:30 (w/w) SP/PLA were prepared. For some blends, 1, 2, 3, and 5 phr PEOX (on the basis of total weight of dry SP and PLA) were added to study the compatibilization effect.

Preparation of Test Specimens. Standard tensile (ASTM D638, type III) test samples were prepared by injection molding (Sumitomo SE 50D) of the previously prepared blends. The temperatures of the three zones of the barrel and nozzle were set at 150, 165, and 170 °C, respectively. The mold temperature was 40 °C, and the cycle time was 40 s. These specimens were also use for thermal analysis, phase morphology, and water absorption testing.

Mechanical Properties. All the tensile samples were conditioned in 50% relative humidity (RH) and 23 °C for 7 days prior to tensile testing. The testing was performed on an 8.9 kN, screw-driven universal testing machine (Instron 4466) equipped with a 10 kN electronic load cell and mechanical grips. The tests were conducted at a crosshead speed of 5 mm/min with the strain measured by a 25 mm extensiometer (MTS 634.12E-24). All tests were carried out according to the ASTM standard, and five replicates were tested for each sample to obtain an average value.

Thermal Analysis. Thermal analysis was performed on the injection molded samples. The samples were shaped into strips ($15 \times 3 \times 1.3$ mm^3) using a milling machine. Unless stated otherwise, all specimens were conditioned in 50% RH and 23 °C for 7 days prior to testing. Dynamic mechanical analysis (DMA) was conducted using a Perkin-Elmer DMA-7 (Norwalk, CT) with a three-point bending fixture. The samples were scanned from −50 to 180 °C at 2 °C/min with a fixed oscillation frequency of 1 Hz. The static and dynamic forces were 0.0020 and 0.0022 N, respectively. Each sample was analyzed in duplicate. Differential scanning calorimetry (DSC) was conducted on a Mettler Toledo DSC 822e instrument. The specimens were crimp-sealed in 40 μL aluminum crucibles. All specimens were heated from 20 to 185 °C at 10 °C/min and kept isothermal for 1 min and then cooled to 25 °C at 10 °C/min. To study the effects of moisture on glass transition and crystallization of PLA, specimens were equilibrated in chambers of different RH at 23 °C for 7 days. Saturated salt solutions of LiCl, $MgCl_2$, $Mg(NO_3)_2$, NaCl, and KNO_3, giving RH of 11, 32, 50, 75, and 93%, respectively, were used for this study.[2]

Rheological Analysis. Dynamic rheological properties of the SP/PLA blends were assessed using a strain-controlled rheometer (Rheometric Scientific, RDA III). Tests were performed on the extruded blend samples using a parallel-plate geometry ($d = 25$ mm). A dynamic time sweep test was conducted to assess the thermal stability of the blends. Considering the susceptibility of thermal degradation of soy protein and the melting temperature of PLA, the testing temperature was set at 175 °C. PLA extruded at the same condition as the blends was used as a control. The sample was loaded between the parallel plates and melted at 175 °C for 3 min. The parallel plates subsequently compressed the sample to 1 mm thick prior to each test. A strain sweep test was initially conducted to determine the linear viscoelastic region of the materials. A dynamic frequency sweep test was performed to determine the dynamic properties of the blends. The strain and frequency range used during testing were 5% and 0.1−500 rad/s, respectively. Steady-state shear tests at the same temperature were also conducted to investigate the viscosity−shear rate relationship. The shear rates ranging from 0.05 to 50 l/s were employed.

Phase Morphology. Scanning electron microscopy (SEM) was used to examine the phase structure of the blends. The injection molded tensile specimens were cryofractured in either a longitudinal or transverse direction of the specimens. To obtain a better observation of the phase structure, some fractured surfaces were extracted with chloroform and then rinsed with hot water to remove the PLA phase or extracted with a solvent to remove the SP phase. The solvent for SP extraction was prepared by making a solution of 0.1 M $NaSO_3$ and 8 M urea using a buffer containing 2.6 mM KH_2PO_4 and 32.6 mM K_2HPO_4.[29] The PLA extraction with chloroform took a few minutes, while the SP extraction with a buffer solution took from 10 min to several hours, with longer times needed for SPC/PLA blends and blends with higher PLA contents. The extracted surfaces were dried and sputter coated with gold prior to examination.

Water Absorption. A water absorption test was conducted following the ASTM D570-81. The samples were dried at 50 °C for 24 h prior to the test and then immersed in distilled water at room temperature. The percentage weight gain was taken as the water absorption value. Five replicates were tested for each sample.

Molecular Weight Measurements. The PLA molecular weight was monitored by gel permeation chromatography (GPC) before and after compounding. The GPC system was equipped with a Hitachi L-6200A gradient pump, a Polymer Labs PL-Gel 5 μm mixed column, and a Hitachi L-3350 RI detector. Chloroform was used as the eluent at a

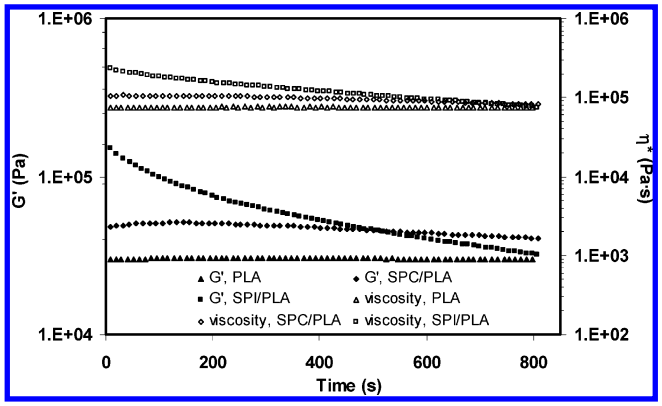

Figure 1. Dynamic time sweep of PLA and SP/PLA (30:70) blends. $\omega = 2$ rad/s, strain = 5%, and temperature = 175 °C.

flow rate of 1 mL/min. The GPC system was calibrated using monodisperse polystyrene standards.

Results and Discussion

Rheological Properties. Figures 1−3 give the dynamic rheological properties of PLA and its SP blends. At 175 °C, PLA showed a constant viscosity (complex) and storage modulus during the entire experimental time. SPC/PLA blends also maintained almost constant values up to 400 s. These results suggest good thermal stability of PLA and its SPC blends within the experimental period (Figure 1). On the other hand, the viscosity and storage modulus of SPI/PLA blends experienced an obvious decrease with time, indicating thermal degradation of the sample. It is known that PLA is susceptible to hydrolysis. The water added to SP during the blend preparation would hydrolyze PLA. GPC analysis showed an approximate 13% decrease in the weight-average molecular weight of PLA after extrusion blending for both SPI/PLA and SPC/PLA blends. It was also noticed that although the extrudates were carefully dried prior to injection molding, the molecular weight of PLA further decreased in the subsequent injection molding process, with SPI/PLA showing a larger decrease than SPC/PLA. It is not clear if this is due to the high content of soy protein in SPI, which directly caused PLA degradation, or to the degradation products of soy protein that accelerated PLA degradation. Nevertheless, rheological testing revealed that the viscosity of the blend system was substantially higher than that of neat PLA, and SPI/PLA blends showed higher viscosity than SPC/PLA blends (Figures 2a and 3).

PLA displayed terminal behavior ($G' \propto \omega^{1.64}$ and $G'' \propto \omega$) very close to the theoretical prediction ($G' \propto \omega^2$ and $G'' \propto \omega$) for a typical narrow distribution linear polymer (Figure 2b,c). Blending SP with PLA caused a drastic deviation of the terminal behavior and resulted in much higher η^*, G', and G'' in the low frequency range and η at low shear rates. These changes indicated that the addition of SP greatly increased the molecular interactions of the blend system, and the movement of molecular chains was hindered remarkably. This high intermolecular interaction was likely attributed to the high polarity of SP. Rheology tests were not operated on preformulated SP because the SP or even SP/PLA blends with 30% PLA were not able to flow and be pressed properly between the parallel plates of the rheometer under the experimental conditions. The high viscosity and poor flowability of SP was due to the lack of a large amount of plasticizer(s).

Phase Morphology. Figures 4 and 5 show the phase structures of SPI/PLA and SPC/PLA blends, respectively, with

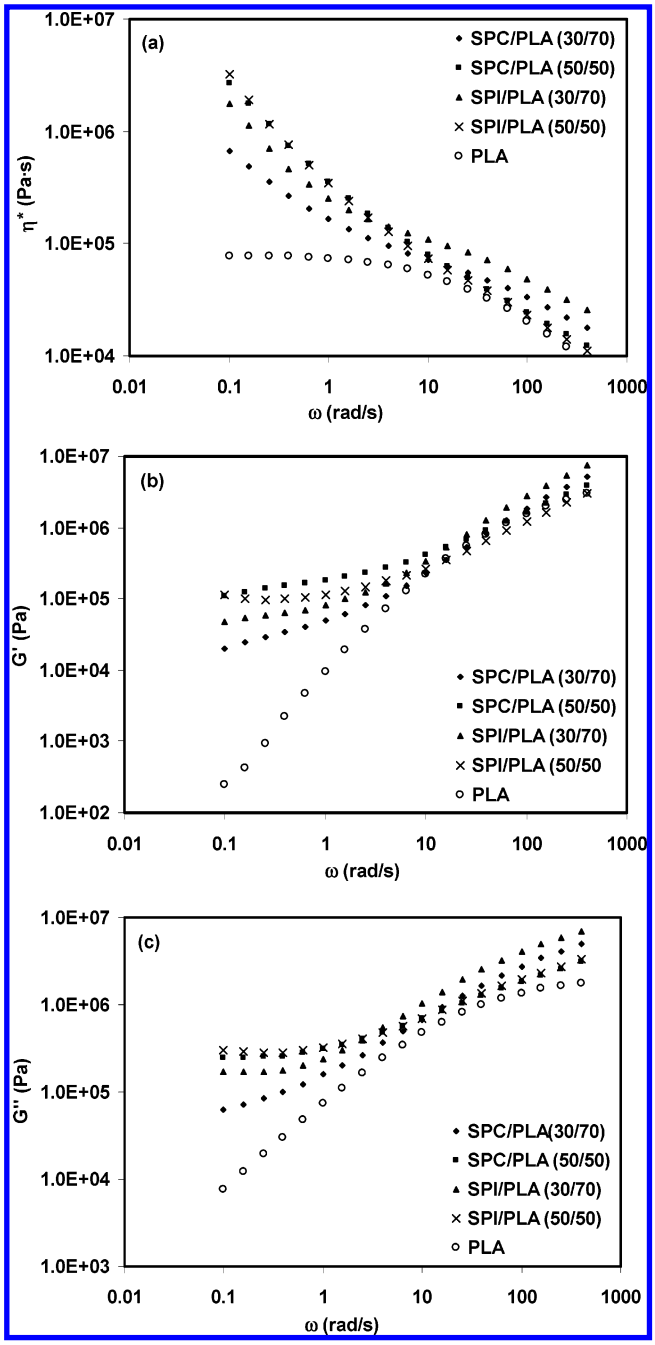

Figure 2. Dynamic frequency sweep of PLA and SP/PLA blends. Strain = 5% and temperature = 175 °C.

a SPI (or SPC)/PLA ratio varying from 30:70 to 70:30 (w/w). These SEM micrographs were taken on the cryofractured surfaces that had been extracted with either buffer solution or chloroform to expose the PLA or SP domain, respectively (see Experimental Procedures). In general, SEM micrographs of SPI/PLA blends revealed severely coarsened phase structures for both domains, while SPC/PLA blends showed a much finer phase structure for both domains. In fact, the phase coarsening in SPI/PLA blends revealed in this study showed a similarity with other SP blend systems.[4,13,30] The phase structure of SPI/PLA blends was complex (Figure 4). The SPI domain appeared to be continuous in all three blends, while the PLA domain percolated in the SPI phase. It is well-recognized that the morphology of a polymer blend depends on several factors, including interfacial adhesion, phase volume ratio, viscosity ratio of the components, and processing conditions.[31−37] The main

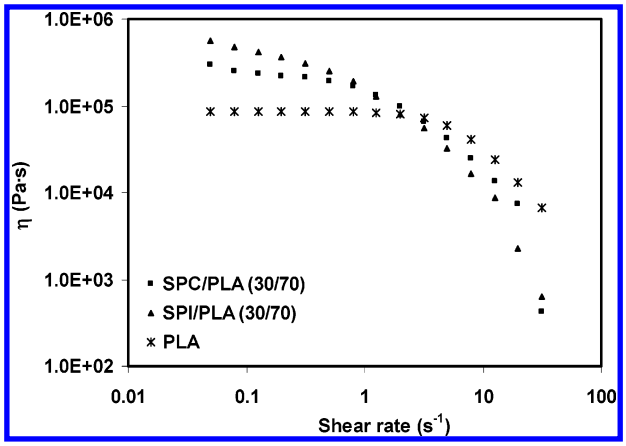

Figure 3. Steady shear viscosity of SP/PLA blends. Temperature = 175 °C.

mechanism governing the morphology development is the balance between droplet break-up and coalescence.[32] SPI contains ca. 90% soy protein, which is highly polar and hydrophilic, while PLA is hydrophobic. This leads to poor interfacial adhesion between the two phases. The low interfacial adhesion, as well as high viscosity disparity between SPI and PLA, played an important role in the phase coarsening.[32,33,36,37] Although the water contained in preformulated SP gelated and plasticized SP when heated, the viscosity of SP was still much higher than PLA as observed from rheology tests. The SP/PLA viscosity ratio is therefore believed to be much larger than 1, which is not favorable for a fine phase dispersion in a blend system.[37] The viscosity of the SPI component was so high that the coalescence of SPI outperformed its break-up during processing, and hence, it tended to remain as a continuous phase.[32,37] On the other hand, the relatively low viscous PLA domain was easy to break-up and disperse in the SPI domain, and once it dispersed in the highly viscous SPI phase, it was difficult for it to diffuse in SPI.[32]

In contrast, SPC/PLA blends exhibited a much finer co-continuous phase structure in the SPC/PLA ratio (w/w) ranging from 30:70 to 70:30 (Figure 5). This fine phase structure of SPC/PLA blends might be the result of improved interfacial adhesion between the two phases and lower viscosity of SPC phase than that of SPI phase due to weaker intermolecular charge−charge interactions. Since SPC contains much less protein (ca. 50%) than SPI (ca. 90%) but more carbohydrates, the interfacial adhesion between SPC and PLA might be higher and facilitate the formation of a fine phase structure.[31] The better compatibility between SPC and PLA than that between SP and PLA was proven in the DMA testing discussed next.

Figure 6 shows PLA phase morphology in the blends along the longitudinal direction. It is clear that the PLA phase was aligned along the flow direction, with SPI/PLA showing a higher degree of orientation than SPC/PLA. This is probably due to the higher viscosity of SPI than that of SPC, which kept the shear deformed PLA phase from recovery. The effect of PEOX on phase morphology is illustrated in Figure 7. The samples were cryofractured without etching. The SPI/PLA blend without PEOX showed large domain sizes, and the addition of PEOX resulted in a finer structure, indicating improved mixing. In contrast, the SPC/PLA blend showed a more homogeneous phase structure than SPI/PLA, and the addition of PEOX further improved interfacial adhesions so that local plastic deformation (surface roughening) was observed.

Mechanical Properties and Water Absorption. The properties of a polymer blend are strongly influenced by its morphology. Table 1 shows the mechanical properties and water absorption of SP/PLA (70:30 w/w) blends containing different amounts of PEOX. The tensile strength of the SPI/PLA blend without a compatibilizer was 12.4 MPa, which was even lower than that of highly plasticized SP sheets (e.g., 14.1 MPa for a sheet containing 23% glycerol).[2] This result suggested poor compatibility between SPI and PLA. The addition of 1 phr PEOX resulted in a significant increase in tensile strength and a decrease in water adsorption, suggesting that PEOX functioned as a compatibilizer for SPI/PLA blends. However, the further increase of PEOX concentration led to only slight improvements in strength and water resistance of the SPI/PLA blends. Adding PEOX to the SPC/PLA blend also improved its performance, but to a lesser extent compared to SPI/PLA blend. For uncompatibilized blends, SPC/PLA had a higher tensile strength (19.3 vs 12.4 MPa) and modulus (4.43 vs 3.96 GPa) than SPI/PLA, indicating a better compatibility in the former system. On the other hand, the high moduli and low elongations of both blends were largely unaffected by the compatibilizer, reflecting the characteristic high rigidity for both PLA and SP.

Increasing the PLA concentration in the blends resulted in increases in tensile strength (Figure 8a), with SPC/PLA blends demonstrating a higher tensile strength at all concentrations than SPI/PLA. The superior performance of SPC/PLA blends to SPI/PLA blends was likely attributed to the better compatibility between PLA and SPC than between PLA and SPI. These results are consistent with the findings in the phase morphologies of these two blend systems, where SPC blends demonstrated a much finer co-continuous phase structure than SPI blends. The higher carbohydrate content in SPC than SPI might contribute to the better compatibility between SPC and PLA and leads to finer phase structures and a higher tensile strength. Because both PLA and SP are rigid polymers and show brittleness without proper plasticization, all the SP/PLA blends showed low elongation at break and low tensile toughness. SEM micrographs (not shown) of the tensile fracture surfaces of the blends all illustrated typical brittle failure. The blends containing 70 parts of SP generally showed poor water resistance, absorbing more than 12 wt % of water within 2 h (Table 1); water absorption test beyond a 2 h immersion were not recorded for these blends because of the severe swelling and deformation of the samples. Nevertheless, water absorption was dramatically decreased when the SP concentration was reduced (Figure 8b). With 30 parts of SP in the blends, the SPC/PLA blend demonstrated superior water resistance to the SPI/PLA blend. For example, the SPC/PLA (30:70 w/w) blend absorbed only 1.7 and 4.55 wt % of water for a 24 and 72 h immersion, respectively, while for the same periods, the SPI/PLA (30:70 w/w) blend absorbed 2.9 and 16.6 wt % of water, respectively.

Dynamic Mechanical Properties. As the addition of PEOX resulted in a finer phase structure of the blends (Figure 7) and increased tensile strength and water resistance (Table 1), particularly for the SPI/PLA blends, its addition also influenced the dynamic mechanical properties of the blends. Neat PLA was almost amorphous after sample preparation (see Crystallization). It became very soft when the temperatures were above its α-transition (peak at ca. 70 °C) and hence showed a large damping peak at the transition in a DMA thermogram (inset in Figure 9a). Since a severe deformation (bended) of the neat PLA specimen occurred at temperatures above its T_g, the scanning was therefore stopped at 80 °C. The damping spectrum of SPI (containing 2 phr glycerol) showed a steady increase in temperature from ca. 110 °C but did not yield a typical α-transition peak within the experimental temperature range

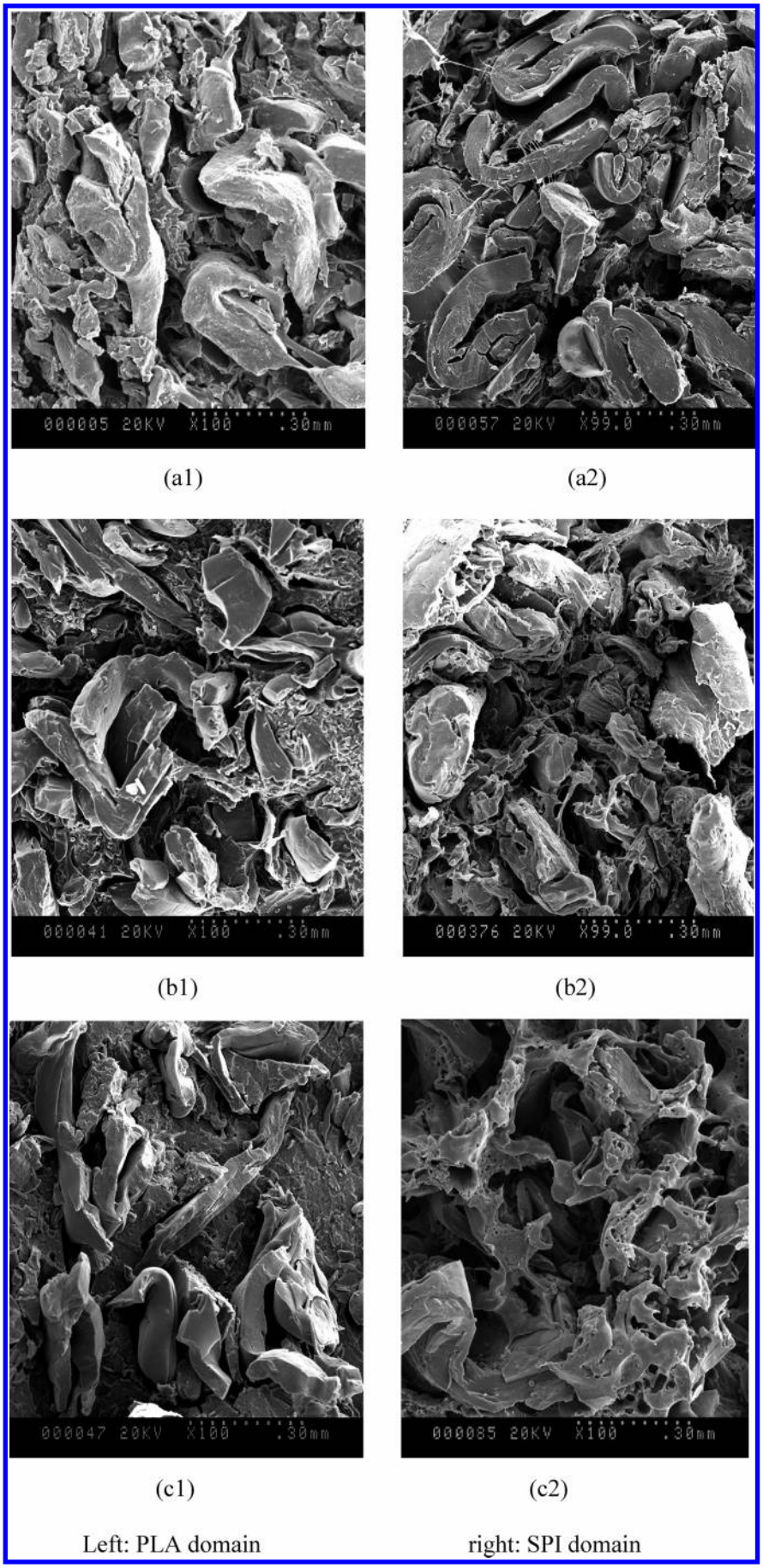

Figure 4. SEM micrographs of SPI and PLA phases in blends containing 3 phr PEOX. (a1 and a2) SPI/PLA = 70:30 (w/w); (b1 and b2) SPI/PLA = 50:50 (w/w); and (c1 and c2) SPI/PLA = 30:70 (w/w). Samples were fractured in transverse directions; surfaces were etched with a buffer solution to remove SP or with $CHCl_3$ to remove PLA.

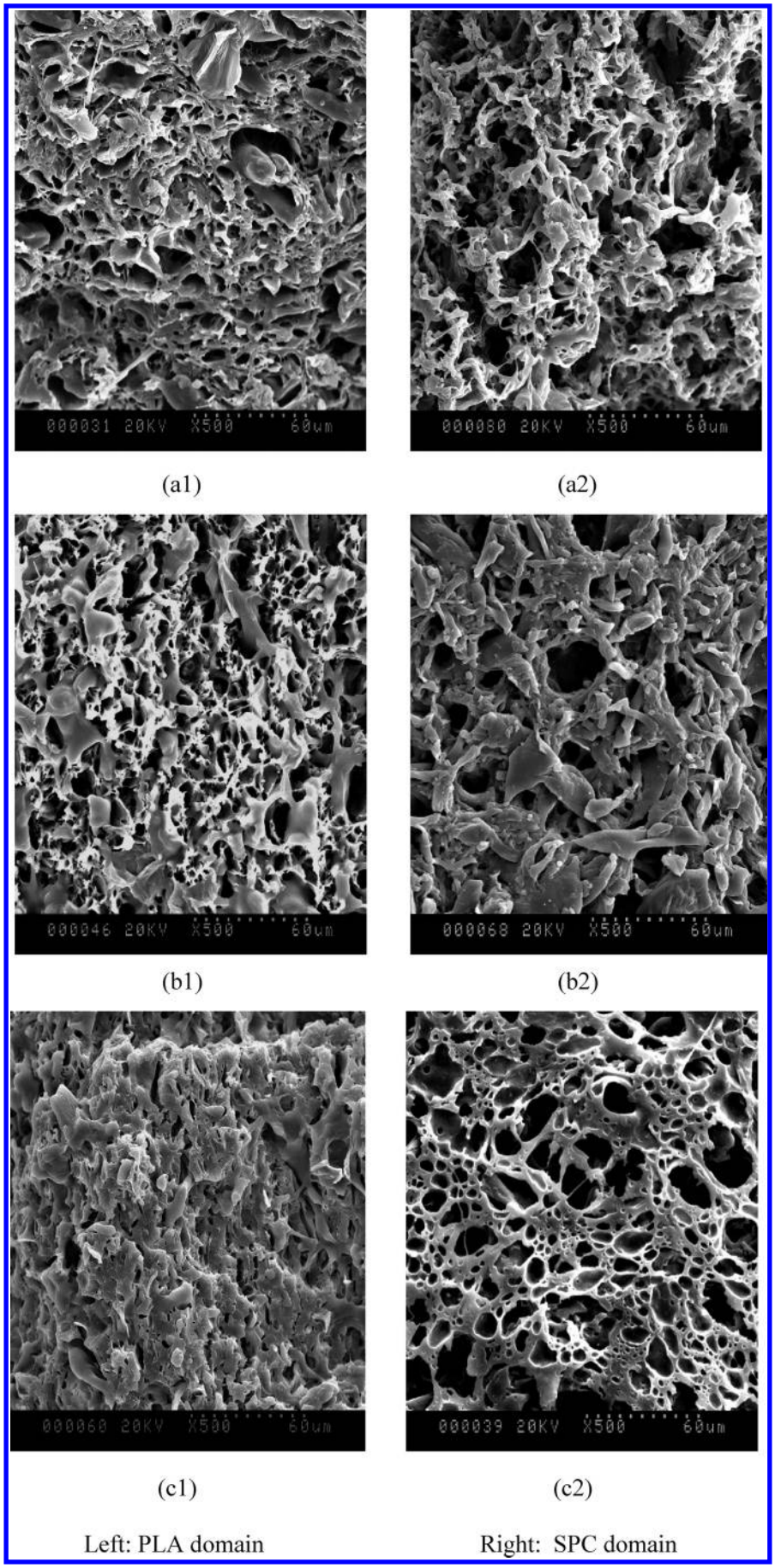

Figure 5. SEM micrographs of SPC and PLA phases in blends containing 3 phr PEOX. (a1 and a2) SPC/PLA = 70:30 (w/w); (b1 and b2) SPC/PLA = 50:50 (w/w); and (c1 and c2) SPC/PLA = 30:70 (w/w). Samples were fractured in transverse directions; surfaces were etched with a buffer solution to remove SP or with $CHCl_3$ to remove PLA.

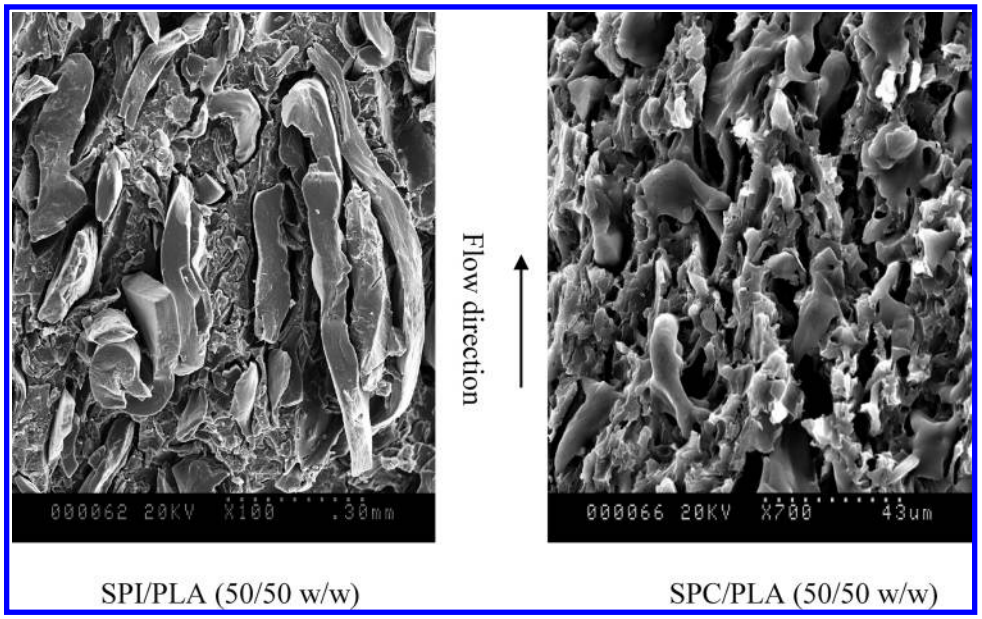

Figure 6. SEM micrographs of PLA phase in different blends containing 3 phr PEOX. (Surfaces were extracted with a solvent to remove SP.) Samples were fractured in longitudinal directions; surfaces were etched with a buffer solution to remove SP.

Table 1. Mechanical Properties of SP[a]/PLA Blends and Effect of Poly(2-ethyl-2-oxazoline)

sample	PEOX (phr)[b]	strength (MPa)	elongation (%)	modulus (GPa)	water uptake (%, 2 h)
SPI/PLA (70:30 w/w)	0	12.4 ± 2.0	1.3 ± 0.1	3.96 ± 0.22	18.2 ± 1.6
	1	18.1 ± 2.0	1.8 ± 0.3	3.82 ± 0.29	14.8 ± 0.2
	3	19.4 ± 1.5	1.9 ± 0.1	3.73 ± 0.25	12.7 ± 1.0
	5	20.1 ± 1.7	1.9 ± 0.1	3.75 ± 0.18	12.1 ± 1.2
SPC/PLA (70:30 w/w)	0	19.3 ± 0.6	1.7 ± 0.1	4.43 ± 0.28	15.1 ± 1.0
	1	20.3 ± 1.0	1.8 ± 0.1	4.52 ± 0.26	13.8 ± 0.4
	3	22.0 ± 1.2	1.9 ± 0.1	4.38 ± 0.16	15.5 ± 0.5
	5	22.5 ± 1.2	2.1 ± 0.2	4.25 ± 0.10	15.1 ± 0.4
PLA		63.1 ± 1.6	3.8 ± 0.4	3.43 ± 0.09	

[a] SP was based on its dry weight in the formulated mixture (see Experimental Procedures). [b] PEOX is added on the basis of per hundred resin (total weight of SP and PLA).

(inset in Figure 9a). Accordingly, the E' of SPI displayed an obvious drop in the same temperature range (Figure 9b). Previous studies indicated that the T_g of dry SPI is in the vicinity of 140 °C[2,38] and that its value could be lowered by moisture absorption[2] or by adding plasticizer(s).[2,3,6,11,38] Therefore, it is believed that the changes in tan δ and E' of the neat SPI in this region were due to the glass transition of SP. The large deviation of the decrease in E' ($\sim$ 2 times) for the neat SP during the α-transition from the decrease in E' ($\sim 10^3$ order) for conventional plastics in the same transition might be the consequence of a certain degree of cross-linking of SP[29] under the conditions in this study and strong molecular interactions of SP. It looks as if the neat SP showed higher damping (tan $\delta > 0.5$) values up to 110 °C than neat PLA, which displayed a fairly low damping (tan $\delta < 0.1$) except at its α-transition ($\sim$60−85 °C).[39,40,42] The damping peak of PLA in the blends was greatly reduced because the SP component was still in the glassy state in the α-transition range of PLA. In Figure 9a, two transition peaks can be observed for SPI/PLA blends without PEOX. The first one corresponds to the α-transition of the PLA domain, and the second peak is likely attributed to the α-transitions of the SPI domain in the blends. With the addition of PEOX, the α-transition of the SPI domain was shifted toward to lower temperatures (i.e., the α-transition temperature of the SPI domain was shifted from ca. 100 °C (peak value, no PEOX) to ca. 93 °C (peak value, 5 phr PEOX), while that of the PLA domain showed little change with PEOX). This change might be due to the improved compatibility between the two domains with the addition of PEOX. It might also be the consequence of miscibility of SPI and PEOX. PEOX is amorphous with a T_g of ca. 37 °C. The SPI/PEOX (90:10 w/w) plasticized with 15 phr glycerol blend displayed a single T_g at ca. 88.5 °C (DSC analysis), while the PLA/PEOX blends showed two distinct glass transitions corresponding to that of individual components (data not shown). It is interesting to note that the blends demonstrated a higher E' than both PLA and SPI at temperatures below the α-transition of the PLA domain. This change might be related to the lower equilibrium moisture absorption of SP in the blends than SP in the neat form, making the SP stiffer in the blends than in the neat form.

Figure 10 demonstrates the effect of the moisture level in the blends on the dynamic mechanical properties. It is reasonable to believe that most of the moisture in the blend would remain in the SP phase for its high polarity, and reducing the moisture level would decrease the SP damping peak and shift it to a higher temperature. As compared with specimens conditioned at 50% RH, which contained ca. 4 wt % moisture (based on SPI weight), the damping peak of SPI for the specimen conditioned at 0% RH that contained ca. 0.5 wt % moisture decreased dramatically (Figure 10a) and shifted outward. Accordingly, the E' of the latter in the same temperature range was higher than the former, indicating a more elastic response. Furthermore, the specimen conditioned at 50% RH was scanned a second time after cooling from the first scan. Since the

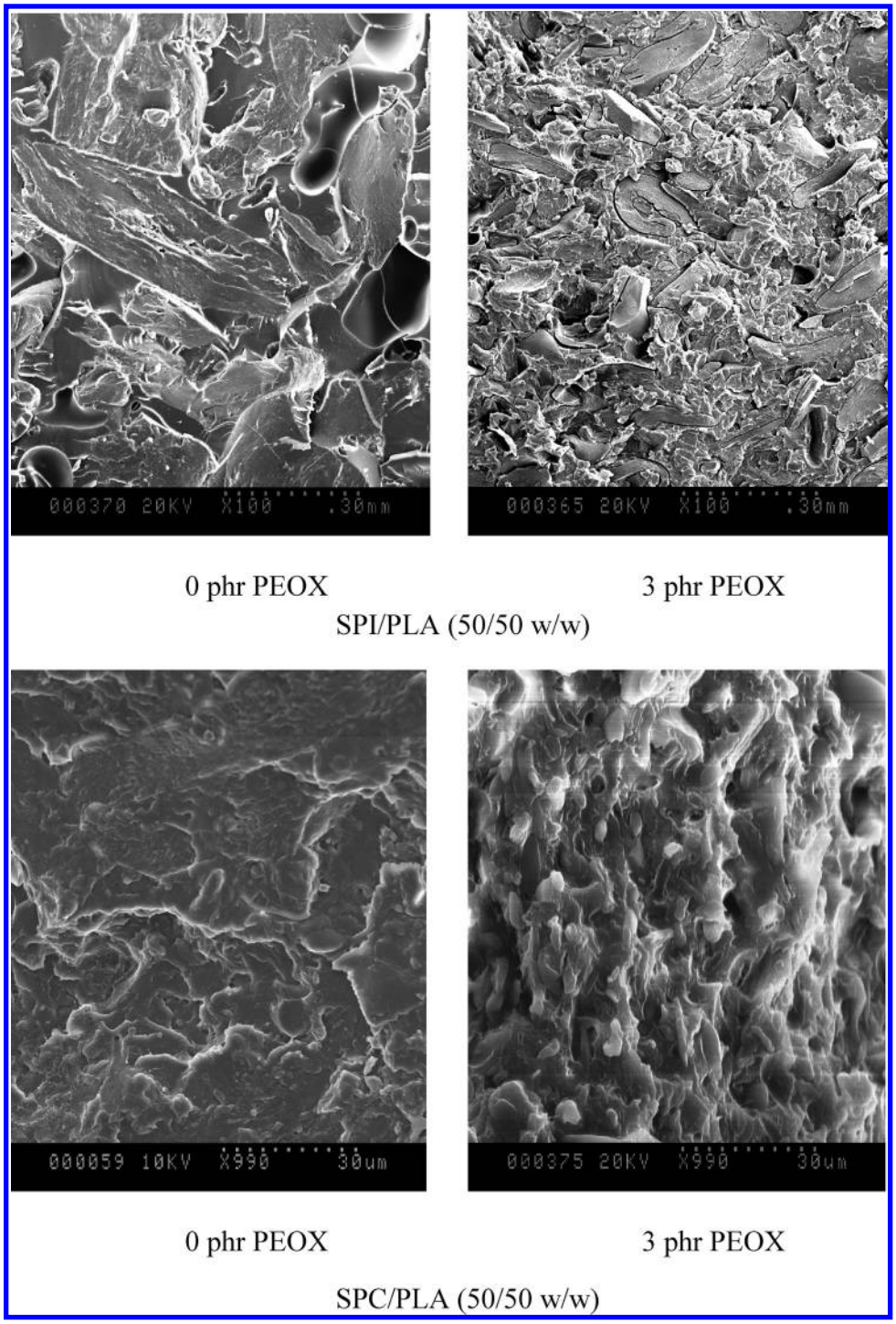

Figure 7. Cryo-fractured surface without etching, showing the effect of PEOX on morphologies of the SP/PLA (50:50 w/w) blends. Samples were fractured in transverse directions.

moisture in the blend was almost completely evaporated during the first scan, the α-transition of SPI in the second scan appeared at a higher temperature and probably overlapped with the melting transition of PLA. The deformation of the PLA phase was substantially restricted after PLA crystallization and SPI stiffening during the first scan. Consequently, the damping of PLA was greatly reduced in the second scan as shown in Figure 10a. Likewise, the loss of E' with temperature was also remarkably reduced since PLA crystallized and the SPI phase became stiffer. In Figures 9−11, E' reached a minimum between the two α-transitions and then recovered as the temperature increased further. This is attributed to the cold crystallization of PLA that occurred within this temperature range during a DMA temperature scan.[17,18,41] The cold crystallization of PLA was confirmed by DSC thermograms (Figure 12) as discussed in the next section. The lack of a similar recovery in E' in the second scan of DMA of the blend (Figure 10b) further supports this argument because the cold crystallization had been completed in the first scan. As compared with SPI/PLA blends, the SPC/PLA blends exhibited higher compatibility as demonstrated by the closer and broader damping peaks (Figure 11). The addition of PEOX in the SPC/PLA blend had little effect on the transitions. These results are consistent with the mechanical properties reported in Table 1.

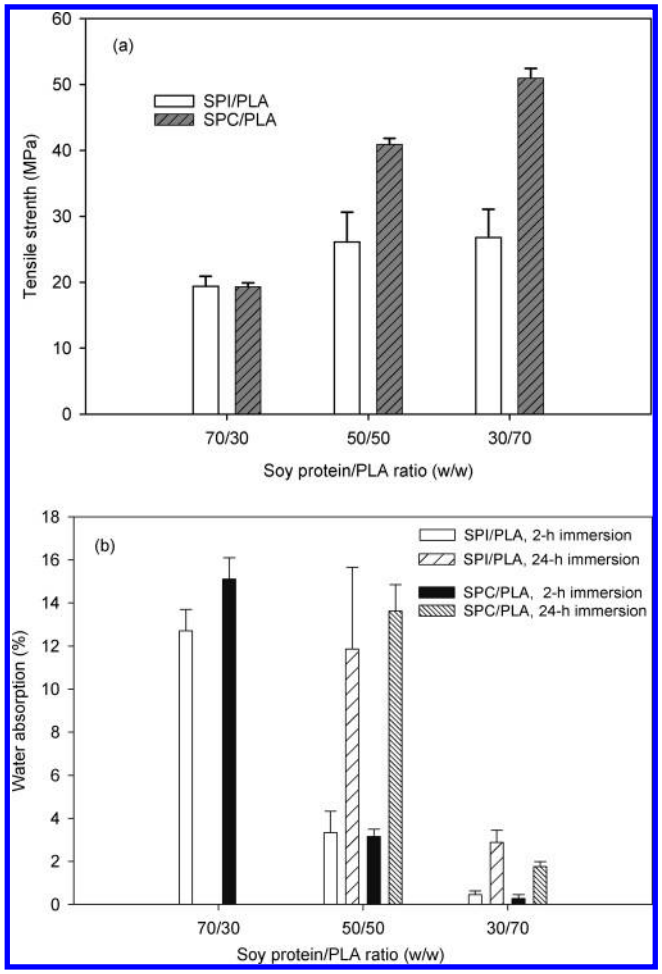

Figure 8. Tensile strength and water absorption of SP/PLA blends with different SPC (or SPI)/PLA ratios.

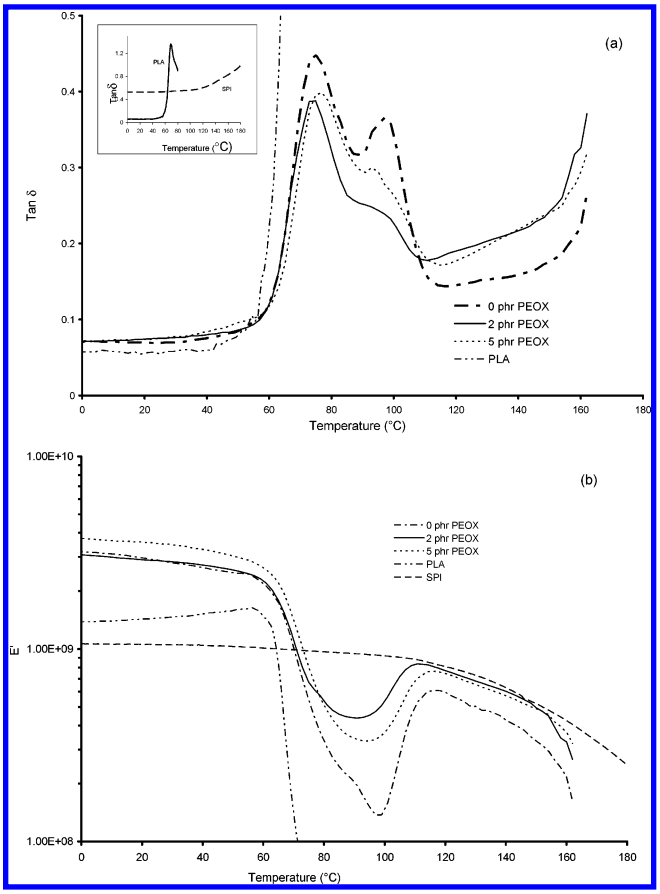

Figure 9. Effect of PEOX content on dynamic mechanical properties of SPI/PLA (70:30 w/w) blends.

Crystallization. Figure 12 shows the DSC thermograms of SP/PLA blends; the testing samples were from the injection molded tensile specimens. Table 2 gives the summary of the DSC results from the first heat scan, revealing the glass transition and crystallization status of the PLA component of the blends in the injection-molded specimens. An exothermic peak, attributed to the cold crystallization during the temperature increase,[17,18,39−42] was observed for each blend and the neat PLA. The recovery in the storage modulus found in DMA tests (Figures 9−11) coincided with this peak. As compared to neat PLA, the cold crystallization of PLA in the blends took place at much lower temperatures and exhibited narrower peak widths. Furthermore, PLA in the blends showed a substantially higher ΔH_{cc} (or ΔH_m) than that of neat PLA (Table 2). These results suggest that SP induced and accelerated the crystallization of PLA and substantially increased the crystallinity of PLA. The very similar ΔH_{cc} and ΔH_m values for neat PLA indicate that PLA was primarily amorphous since it was not able to crystallize when it was rapidly cooled during the injection molding. On the other hand, all blends showed larger ΔH_m than ΔH_{cc} values, indicating a certain degree of crystallinity of the PLA in the blends promoted by the presence of SP. The bimodal endothermic transition (∼140−160 °C) is the melting of PLA in the blend. The melting peak at lower temperatures (∼140−150 °C) was due to the melting of crystals with less perfection in the boundary regions, which subsequently recrystallized and remelted at a higher temperature.[42]

The PLA in all blends (Table 2) showed a slightly lower T_g (∼ 1.4−4 °C) than that of neat PLA. In addition, the cold crystallization temperature (T_{cc}) and the melting temperature (T_m) of PLA in the blends showed similar decreases in comparison with that of neat PLA. These are mainly attributed to the residual moisture in the blends. The absorbed (or residual)

Table 2. Cold Crystallization and Melting of PLA in the Molded Samples of Different SP/PLA Blends[a] Containg 3 phr PEOX[a]

				cold crystallization		melting T_m (°C)		
blends	symbol	ratio (w/w)	T_g (°C)	T_{cc} (°C)	ΔH_{cc}[b] (J/g)	1	2	ΔH_m[b] (J/g)
SPC/PLA	a	70:30	58.3	113.2	21.2	146.2	153.2	26.8
	b	50:50	57.8	105.9	27.3	143.8	152.9	33.1
	c	30:70	57.9	104.1	26.0	144.6	153.9	28.4
SPI/PLA	a′	70:30	54.7	103.3	24.2	141.7	153.8	30.5
	b′	50:50	56.9	100.8	23.9	142.3	151.6	29.3
	c′	30:70	54.9	94.5	28.4	140.7	151.6	33.4
Neat PLA	d		59.3	123.7	12.6		154	12.7

[a] Data are baded on the first heating scan of the samples prepared by injection molding. [b] Data corrected for the percentage of PLA in the blend.

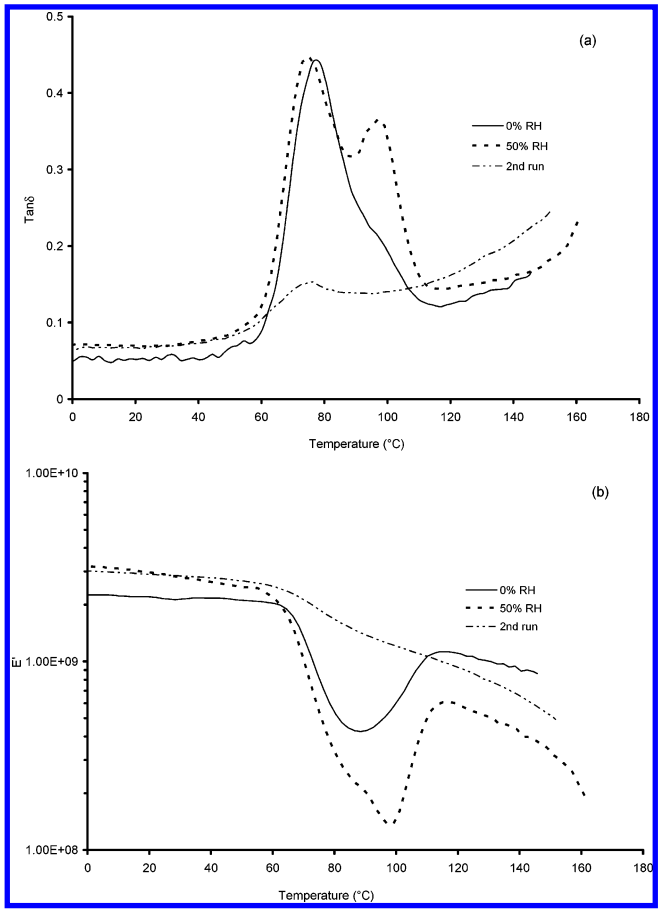

Figure 10. Effect of moisture level on dynamic mechanical properties of the SPI/PEOX/PLA (70:3:30 w/w/w) blend.

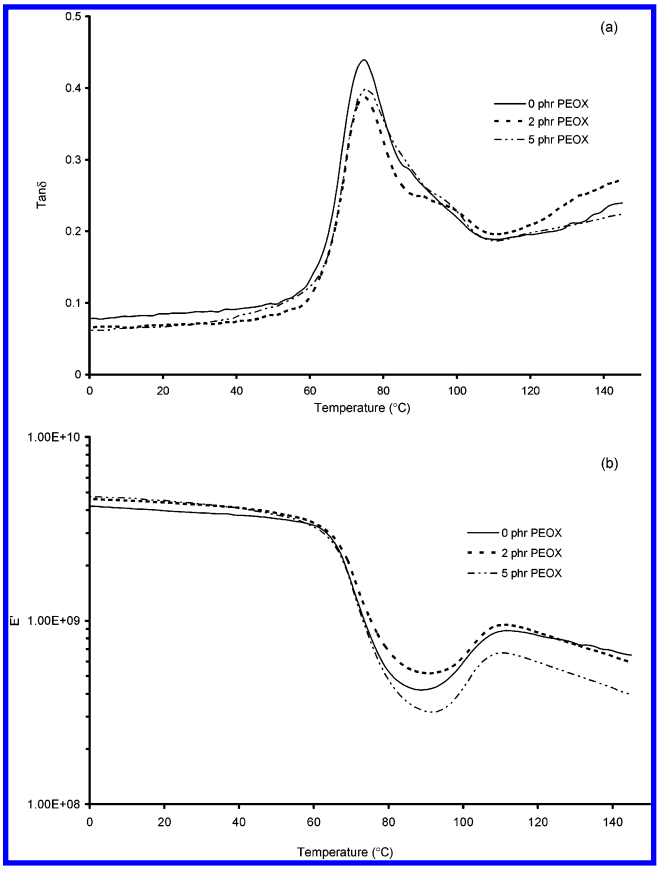

Figure 11. Effect of PEOX content on dynamic mechanical properties of SPC/PLA (70:30 w/w) blends.

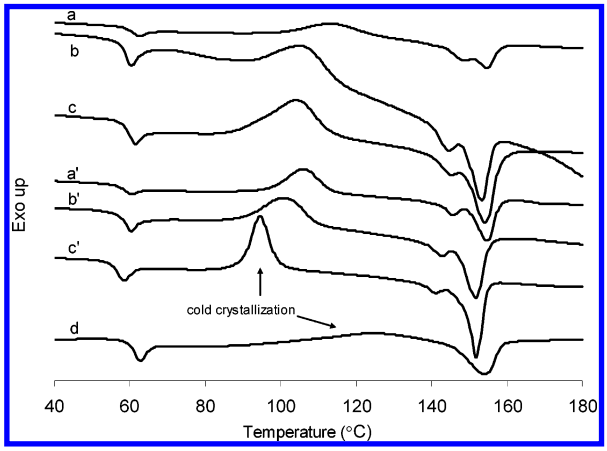

Figure 12. DSC thermograms of different SP/PLA blends. Thermograms were based on the first heat scan performed on samples from injection molded specimens. The sample compositions are listed in Table 2.

moisture plasticizes PLA molecules and increases the flexibility of the molecules, resulting in lowered crystallization and melting temperatures. Further support for this argument can be found in Figure 13, which gives the DSC thermograms (first heat scan) of the SPI/PLA (70:30) blend containing 3 phr PEOX conditioned at environments of different relative humidity for 7 days. The DSC results clearly indicated that the T_g, T_{cc}, and T_m of PLA in the blends decreased continuously with the increase in moisture content (% RH increasing).

Conclusions

SP/PLA blends were successfully prepared by extrusion mixing. SP plastics showed increased flowability and processibility after blending with PLA and could be injection-molded with only small amounts of processing aids. Study of the melt rheology suggested there were strong molecular interactions in the melts of the blends attributed to the SP. The blend system showed substantially higher viscosity than neat PLA, particularly at low shear rates. Investigations of plasticization and formulation will be necessary to optimize process and product properties. A co-continuous phase morphology was found in the SPC/PLA blends with a broad range of compositions. Phase morphology, DMA results, and mechanical properties indicated that SPC had a higher compatibility with PLA than SPI, which resulted in finer phase structures and higher mechanical properties of SPC/PLA blends. The mechanical properties of SPC/PLA blends were enhanced greatly with the increasing PLA contents, while the mechanical properties of SPI/PLA blends demonstrated only limited increases. The presence of PLA components substantially reduced the water absorption of SP. When the SP/PLA ratio was 30:70 (w/w), SPC/ PLA and SPI/PLA blends absorbed only 1.7 and 2.9 wt % water for a 24 h immersion, respectively. PEOX can be used as a compatibilizer in the blends, leading to improved mixing of the two phases. Mechanical properties and water resistance of SP/PLA blends were improved after compatibilization, and the effect was more significant on the SPI/PLA blend than on the SPC/PLA blend. All blend samples showed low elongation at break and failed in brittle fracture in tensile testing, which leaves a space for toughening and plasticization in future investigation. The PLA component in the blends was found to be highly amorphous in

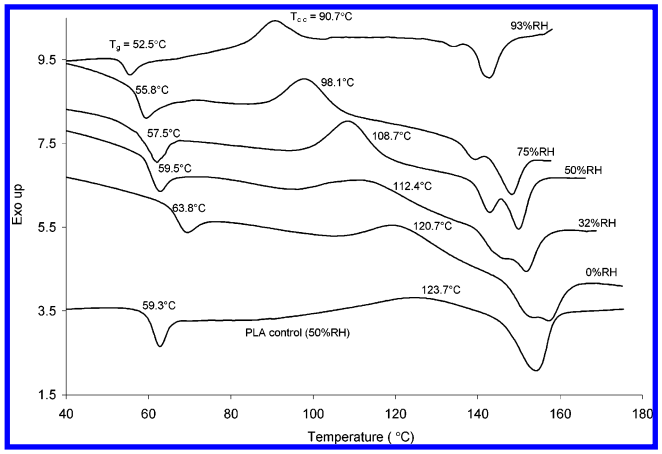

Figure 13. DSC thermograms of the SPI/PEOX/PLA (70:3:30 w/w/w) blend conditioned at different environments. Thermograms were based on the first heat scan performed on samples from injection molded specimens.

injection molded articles due to the rapid cooling in the mold. SP induced and accelerated cold crystallization of PLA in the blends, resulting in a higher PLA crystallinity. This suggests that mechanical properties of the blends could be manipulated under postprocess thermal treatments to suit different applications.

References and Notes

(1) Paetau, I.; Chen, C.; Jane, J. *J. Environ. Polym. Degrad.* **1994**, *2*, 211.
(2) Zhang, J.; Mungara, P.; Jane, J. *Polymer* **2001**, *42*, 2569.
(3) Mungara, P.; Zhang, J.; Zhang, S.; Jane, J. *Protein-based Films and Coatings*; Gennadios, A., Ed; CRC Press: Boca Raton, FL, 2002; pp 621−638.
(4) Wang, C.; Carriere, J.; Willett, L. *J. Polym. Sci., Part B: Polym. Phys.* **2002**, *40*, 2324.
(5) Chang, L.; Xue, Y.; Hsieh, F. *J. Appl. Polym. Sci.* **2001**, *80*, 10.
(6) Wang, S.; Sue, H.; Jane, J. *J. Macromol. Sci., Pure Appl. Chem. A* **1996**, *33*, 557.
(7) Otaigbe, J.; Adams, D. *J. Environ. Polym. Degrad.* **1997**, *5*, 199.
(8) Jane, J.; Wang, S. U.S. Patent 5,523,293, 1996.
(9) John, J.; Bhattacharya, M. *Polym. Int.* **1999**, *48*, 1165.
(10) Zhong, Z.; Su, X. *Polymer* **2001**, *42*, 6961.
(11) Graiver, D.; Waikul, L. H.; Boer, C.; Narayan, R. *J. Appl. Polym. Sci.* **2004**, *92*, 3231.
(12) Wang, N.; Zhang, L. *Polymer* **2005**, *54*, 233.
(13) Chen, Y.; Zhang, L.; Du, L. *Ind. Eng. Chem. Res.* **2003**, *42*, 6786.
(14) Huang, J.; Zhang, L.; Chen, F. *J. Appl. Polym. Sci.* **2003**, *88*, 3284.
(15) Lu, Y.; Weng, L.; Zhang, L. *Biomacromolecules* **2004**, *5*, 1046.
(16) Zheng, H.; Tan, Z.; Zhan, Y. R.; Huang, J. *J. Appl. Polym. Sci.* **2003**, *90*, 3672.
(17) Ke, T.; Sun, X. *J. Appl. Polym. Sci*. **2001**, *81*, 3069.
(18) Wang, H.; Sun, X.; Seib, P. *J. Appl. Polym. Sci*. **2001**, *82*, 1761.
(19) Urayama, H.; Ma, C.; Kimura, Y. *Macromol. Mater. Eng.* **2003**, *288*, 562.
(20) Oksman, K.; Skrifvars, M.; Selin, J. *Compos. Sci. Technol.* **2003**, *63*, 1317.
(21) Aoi, K.; Okada, M. *Prog. Polym. Sci.* **1996**, *21*, 151.
(22) Kobayashi, S.; Kaku, M.; Saegusa, T. *Macromolecules* **1988**, *21*, 334.
(23) Parada, L.; Meaurio, E.; Cesteros, L.; Katime, I. *Macromol. Chem. Phys.* **1998**, *199*, 1597.
(24) Dai, J.; Goh, S.; Lee, S. *Polymer* **1996**, *37*, 3259.
(25) Fang, L.; Goh, S. *J. Appl. Polym. Sci.* **2000**, *76*, 1785.
(26) Lichkus, A.; Painter, P.; Coleman, M. *Macromolecules* **1988**, *21*, 2636.
(27) Ong, C.; Goh, S.; Chan, H. *J. Appl. Polym. Sci.* **1997**, *65*, 391.
(28) Goh, S.; Lee, S.; Zhou, X.; Tan, K. *Polymer* **1999**, *40*, 2667.
(29) Hager, D. *J. Agric. Food Chem.* **1984**, *32*, 293.
(30) Zhong, Z.; Sun, S. X. *J. Appl. Polym. Sci.* **2003**, *88*, 407.
(31) Willemse, R. C.; Posthuma de Boer, A.; van Dam, J.; Gotsis, A. D. *Polymer* **1999**, *40*, 827.
(32) Thomas, S.; Groeninckx, G. *Polymer* **1999**, *40*, 5977.
(33) Everaert, V.; Aerts, L.; Groeninckx, G. *Polymer* **1999**, *40*, 6627.
(34) Walia, P. S.; Lawton, J. W.; Shogren, R. L.; Felker, F. C. *Polymer* **2000**, *41*, 8083.
(35) Li, J.; Ma, P. L.; Favis, B. D. *Macromolecules* **2002**, *35*, 2005.
(36) Rodriguez-Gonzalez, F. J.; Ramsay, B. A.; Favis, B. D. *Polymer* **2003**, 1517.
(37) Denesi, S.; Porter, R. S. *Polymer* **1978**, *19*, 448.
(38) Che, P.; Zhang, L. *Macromol. Biosci.* **2005**, *5*, 237.
(39) Pluta, M.; Galeski, A. *J. Appl. Polym. Sci*. **2002**, *86*, 1386.
(40) Ljungberg, N.; Anderson, T.; Wesslen, B. *J. Appl. Polym. Sci*. **2003**, *88*, 3239.
(41) Liu, X.; Dever, M.; Fair, N.; Benson, R. S. *J. Environ. Polym. Degrad.* **1997**, *5*, 225.
(42) Jiang, L.; Wolcott, M. P.; Zhang, J. *Biomacromolecules* **2006**, *7*, 199.

BM050888P